

# Aroma Release from Solid Droplet Emulsions: Effect of Lipid Type

Supratim Ghosh · Devin G. Peterson ·  
John N. Coupland

Received: 29 April 2007 / Revised: 17 August 2007 / Accepted: 27 August 2007 / Published online: 6 October 2007  
© AOCS 2007

**Abstract** Aroma compounds partition between the different phases of a food emulsion and the headspace but only those in the headspace are perceived. Phase transitions in the lipid droplets profoundly affect the position of the partitioning equilibria and hence headspace aroma concentration. The release of four volatile aroma compounds (ethyl butanoate, pentanoate, heptanoate and octanoate) from eicosane, hydrogenated palm fat or Salatrim<sup>®</sup> emulsions stabilized with sodium caseinate were investigated as a function of fat crystallization, particle size and droplet concentration. For all compounds, the headspace aroma concentration in equilibrium with solid droplet emulsions was significantly higher than that in equilibrium with liquid droplet emulsions. The partitioning of volatile aroma compounds from emulsion does not depend on the type of liquid lipid, however, the interactions between solid lipid droplets and aroma compounds are significantly influenced by the nature of the crystalline fat. Notably, partitioning into the headspace was much lower for solid triglyceride droplet emulsions than for solid alkane emulsions. It was proposed that both residual liquid lipid in solid triglycerides and aroma co-crystallization with solid lipid could

be responsible for higher aroma absorption by solid triglycerides.

**Keywords** Emulsions · Colloids · Lipid chemistry · Lipid analysis · Fat crystallization

## Introduction

The perception of food aroma begins with the release of stimulating volatile molecules from the food and their transport to appropriate receptors in the nose [1, 2]. Aroma release depends on the distribution of aroma compounds in food and in the gas phase above before and during consumption. However, the complex nature of real foods makes it difficult to separate the effect of different interactions on overall aroma release and simple model systems are frequently used. Emulsions are extensively used as model systems because, in addition to being part of real foods, they can be prepared and characterized precisely.

In an oil-in-water emulsion, volatile aroma compounds distribute themselves between the oil droplets, aqueous phase and the surface of the droplets according to the equilibrium partition coefficients (i.e., the ratio of concentrations of aroma compounds in two different phases). The overall partition coefficient of an aroma compound from an emulsion to the gas phase above can also be expressed as a function of individual partition coefficients according to the following mass balance equation [3]:

$$\frac{1}{K_{ge}} = \frac{\phi_o}{K_{ow}} + \frac{1 - \phi_o}{K_{gw}} + \frac{K_{iw}^* \cdot A_s}{K_{gw}} \quad (1)$$

where,  $K_{ge}$ ,  $K_{ow}$  and  $K_{gw}$  are overall gas–emulsion, oil–water and gas–water partition coefficients, respectively,

---

S. Ghosh · D. G. Peterson · J. N. Coupland  
Department of Food Science, The Pennsylvania State University,  
University Park, PA, USA

### Present Address:

S. Ghosh  
School of Nutrition, Ryerson University, Toronto, ON, Canada

D. G. Peterson · J. N. Coupland (✉)  
337 Food Science Building, University Park, PA 16802, USA  
e-mail: coupland@psu.edu

$\phi_o$  oil volume fraction in emulsion and  $A_s$  interfacial area per unit volume of emulsion.  $K_{iw}^*$  is surface binding coefficient defined as the ratio of surface excess concentration, i.e., volume of aroma compound per unit interfacial area, to aqueous concentration. Because the effect of surface binding is much smaller than the effect of partitioning into liquid lipid, the importance of surface binding in emulsions can only be seen where there is no liquid lipid present or the lipid phase is in a solid state [4]. The importance of  $K_{iw}^*$  in partitioning of aroma compounds in emulsions containing solid *n*-eicosane droplets has been shown by Ghosh et al. [3]. It was observed that solid eicosane droplets can significantly absorb aroma compounds at the droplet surface with more effective binding for more hydrophobic compounds. However, these findings are in contrast with observations of Roberts et al. [5] and McNulty and Karel [6] who proposed that only liquid lipid could bind aroma compounds. Another hypothesis proposed by Roberts et al. [5] was that if the aroma compounds were present during fat crystallization they could be trapped inside the solid fat matrix formed on solidification, but again this effect was not observed in our previous study [3]. Possibly these contradicting results may be due to the fact that Roberts et al. [5] used complex triglycerides (hydrogenated palm fat) while our study used pure alkane (*n*-eicosane) [3].

The goal of the present work was to compare the binding of aroma compounds to solid and liquid emulsion droplets prepared from both alkane and triglycerides. The effects of volatile type (an homologous series of ethyl esters), lipid type [*n*-eicosane, hydrogenated palm stearin (HPS), and Salatrim<sup>®</sup>] and droplet size on the partitioning behavior were considered. HPS was tested in this study because it was used previously to study the effect of solid lipid on flavor release [5]. Salatrim<sup>®</sup> (Short And Long chain Acyl TRIGlyceride Molecules) is a family of structured triglycerides prepared with a combination of short (2, 3 or 4 carbon) and long chain (18 carbon) fatty acids. The mixture of chain lengths might accommodate foreign aroma compounds more readily into the crystalline structure during crystallization as proposed by Roberts et al. [5]. In another experiment, volatile partitioning of aroma compounds in two different solid droplet emulsions, before and after fat crystallization, was performed to test for possible aroma entrapment by the solid droplets.

## Materials and Methods

### Materials

Partially HPS (27 Stearin<sup>®</sup>) and Salatrim<sup>®</sup> (Benefat 1H<sup>®</sup>) were the donations from Loders Crokiaan

(Channahon, IL) and Danisco (New Century, KS), respectively. Eicosane and hexadecane was purchased from Fisher Scientific (Springfield, NJ). All other chemicals were obtained from the Sigma Chemical Company (St Louis, MO).

### Emulsion Preparation

Emulsions were prepared by mixing molten lipid (20 wt%) with sodium caseinate solution (2 wt% containing 0.02% thimerosal as an antibacterial agent) using a high-speed blender (Brinkmann Polytron, Brinkmann Instruments Inc., Westbury, NY) for 30 s. The coarse emulsions were then re-circulated through a twin-stage valve homogenizer (Niro Soavi Panda, GEA Niro Soavi, Hudson, WI) at different pressures to achieve a range of droplet sizes. To prevent fat crystallization during emulsion preparation, all ingredients were used at elevated temperatures and the homogenizer was rinsed several times with hot water before and after homogenization. The particle size distributions of the emulsions were characterized by laser diffraction particle sizing (Horiba LA 920, Irvine, CA) using a relative refractive index of 1.15. The emulsions were stored at a temperature greater than 50 °C to prevent fat crystallization. Samples of emulsions were diluted with deionized water to prepare emulsions with different lipid contents.

### Thermal Analysis

The crystallization and melting behaviors of bulk and emulsified lipids were determined using a differential scanning calorimeter (Perkin-Elmer DSC-7, Norwalk, CT). The instrument was calibrated against indium prior to use. Aliquots (~15 mg) of bulk and emulsified lipids were temperature cycled in the DSC from 70 to -40 to 70 °C and 70 to 10 to 70 °C, respectively. The heating and cooling rate was 5 °C min<sup>-1</sup>. The crystallization and melting points of bulk and emulsified lipids were taken from the onset temperature of peaks on the thermogram using Pyris data analysis software (version 3.52, Perkin-Elmer Corporation, Norwalk, CT). All analyses were conducted in triplicate.

### Addition of Aroma Compounds to Emulsions

A stock aroma solution was prepared by mixing four aroma compounds, ethyl butanoate (EB), ethyl pentanoate (EP), ethyl heptanoate (EH) and ethyl octanoate (EO) in a volumetric ratio of 1:2:20:20 and diluting to a 50% solution in

ethanol. The concentrations of the aroma compounds were selected based on their oil–water partition coefficient values so that a quantifiable gas chromatograph peak would be obtained for each compound.

Samples of emulsions were cooled to 10 °C to induce crystallization in the lipid droplets. A stock aroma solution (860  $\mu\text{L L}^{-1}$  of emulsion) was added to each solid droplet emulsions and equilibrated for 24 h at 10 °C. The final concentrations ( $\mu\text{L L}^{-1}$ ) of the aroma compounds in emulsion were: EB 10, EP 20, EH 200, and EO 200. Aliquots (2 mL) of each aroma added emulsion sample was placed into a 20 mL headspace vial (MicroLiter Analytical Supplies, Inc., Suwanee, GA, USA) and were sealed with poly-(tetrafluoroethylene)/butyl rubber septa (MicroLiter Analytical Supplies, Inc., Suwanee, GA, USA). The sealed vials were then temperature cycled to produce (1) solid droplets, (2) liquid droplets and (3) droplets first melted then recrystallized.

1. Solid droplet emulsions (i.e., Solid I samples) were prepared by cooling the samples to 10 °C to ensure complete crystallization of the lipid, then bringing to the experimental temperature specific for the different type of lipids (i.e., 30 °C for *n*-eicosane and 10 °C for HPS and Salatrim<sup>®</sup> emulsions, see Table 1).
2. Liquid emulsion droplets (i.e., Liquid samples) were prepared by heating the Solid I samples (according to temperature scheme of Table 1) to melt the droplets then re-cooling to the experimental temperatures specific for each type of lipid (30, 40 and 50 °C for *n*-eicosane, Salatrim<sup>®</sup> and HPS emulsions, respectively).
3. Finally, recrystallized droplets (i.e., Solid II samples) were made by cooling the Liquid samples back down to 10 °C to induce droplet crystallization and either reheating to 30 °C for *n*-eicosane emulsion or holding at 10 °C for HPS and Salatrim<sup>®</sup> emulsions.

After each phase transition was complete (1 h at the temperature given in Table 1) the samples were maintained at their measurement temperature (according to Table 1) for a minimum of 24 h to allow equilibration prior to HS volatile measurement. At each stage, three separate vials were used to measure the HS volatile concentration and then discarded. Due to their differing melting and crystallization properties, different lipids were studied at different temperatures. Later we will show how it was possible to normalize the data to remove the temperature effect and compare different types of lipid.

It should be noted that “solid” and “liquid” in this work refers to the droplets; the overall emulsions were liquid throughout the experiment and phase transitions in the dispersed phase caused no apparent change in their bulk properties.

#### Headspace Analysis by Gas Chromatograph

Aliquots (1 mL) of the headspace above the emulsion in each vial was sampled using a Combi-Pal autosampler (CTC Analytics, Carrboro, NC) and injected into an Agilent 6890 GC (Agilent Technologies, Palo Alto, CA) equipped with a DB-5 capillary column (30 m  $\times$  0.32 mm i.d. with a 1- $\mu\text{m}$  film thickness) and a flame ionization detector. The operating conditions were as follows: sample was injected in splitless mode; the inlet temperature was 200 °C, the detector temperature was 250 °C, the oven program was 30 °C for 1 min, then increased at 35 °C  $\text{min}^{-1}$  from 30 to 200 °C and held for 2 min; and the carrier constant flow rate was 2.0 mL  $\text{min}^{-1}$  (He). Static HS concentrations were determined from peak areas using a standard calibration curve ( $R^2 = 0.99$ ). All measurements were expressed as the mean and

**Table 1** Emulsion preparation conditions for different lipid types and the temperature program for equilibrium flavor release experiments

Emulsion used	Droplet size category	Homogenization conditions		Mean droplet size ( $d_{32}$ ) ( $\mu\text{m}$ )	Temperature cycle program of emulsions for HS GC analysis		
		Pressure (bar)	Number of passes		Solid droplets (°C)	Melting solid droplets (°C)	Liquid droplets (°C)
Eicosane	Large	110 $\pm$ 10	2	1.04	30	50	30
	Medium	220 $\pm$ 20	2	0.55			
	Small	320 $\pm$ 20	10	0.20			
HPS	Large	110 $\pm$ 10	2	0.91	10	70	50
	Medium	220 $\pm$ 20	2	0.54			
	Small	320 $\pm$ 20	10	0.26			
Salatrim	Large	110 $\pm$ 10	2	1.24	10	50	40
	Medium	220 $\pm$ 20	2	0.50			
	Small	320 $\pm$ 20	10	0.24			

standard deviation of at least three full experimental replicates.

## Results and Discussion

### Physical Properties of the Emulsions

By varying the homogenization conditions, it was possible to manufacture emulsions with different droplet size distributions (Table 1). The droplet size distribution for all the emulsions were unimodal with an average standard deviation of the distribution of  $\sim 0.23 \pm 0.2 \mu\text{m}$ . The emulsions were physically stable over the course of the experiment (i.e., no changes in measured droplet size, no apparent creaming).

The melting and cooling thermograms of the lipids in both their bulk and emulsified forms are shown in Fig. 1. On cooling, both bulk and emulsified lipids crystallized with a single major peak with the exception of bulk eicosane, which showed two exothermic peaks (a shallow peak followed by a sharp one) (Fig. 1a). We were unclear why a pure alkane would consistently show a split exothermic peak, but its presence does not affect the overall goal of the research and was not pursued further. The eicosane and Salatrim<sup>®</sup> samples showed a single peak on heating corresponding to the melting of the crystals (Fig. 1a, c) while HPS had a more complex melting thermogram due to several polymorphic phase transitions (Fig. 1b). According to Kloek et al. [7] the first endothermic peak of HPS (at around 45 °C) corresponded with the melting of the  $\alpha$  polymorph followed by an exothermic peak due to recrystallization to a more stable  $\beta'$  or  $\beta$  polymorph. Finally at around 55 °C, the stable polymorph melted leading to the final exothermic peak (Fig. 1b). At sufficiently high temperature (50 °C for *n*-eicosane and Salatrim<sup>®</sup> and 70 °C for HPS) the solid lipid droplets melted leading to liquid droplet emulsions.

For all lipid types the emulsified lipids crystallized at a lower temperature than the corresponding bulk lipids while the melting points of the bulk and emulsified forms were similar (Fig. 1). The deep supercooling required to initiate crystallization in emulsion lipid droplets has been observed in a wide range of systems and is sometimes attributed to the majority of the lipid being isolated from potential nucleation catalysts and therefore nucleating homogeneously [8]. Eicosane has a deeper supercooling than the two triglycerides (HPS and Salatrim<sup>®</sup>) and this might be due to a difference in the number of potential nucleation catalysts for the triglycerides. The supercooled emulsions were very stable and it was possible to maintain liquid emulsion droplets below their thermodynamic

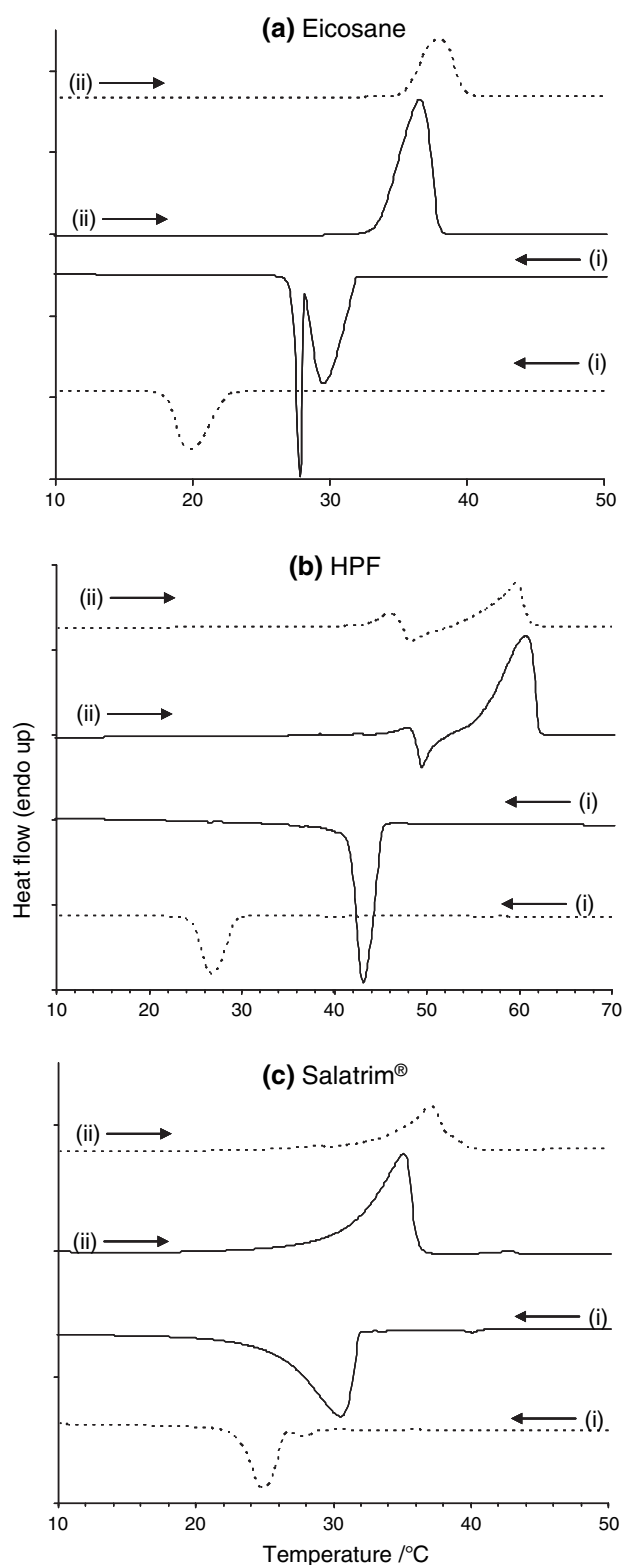


**Fig. 1** Thermogram of bulk (dash line) and emulsified (dotted line) lipids **a** eicosane, **b** HPF and **c** Salatrim<sup>®</sup> during *i* cooling and *ii* heating. Emulsions were 20 wt% lipid stabilized with 2 wt% sodium caseinate solution and was temperature cycled at  $5 \text{ }^\circ\text{C min}^{-1}$

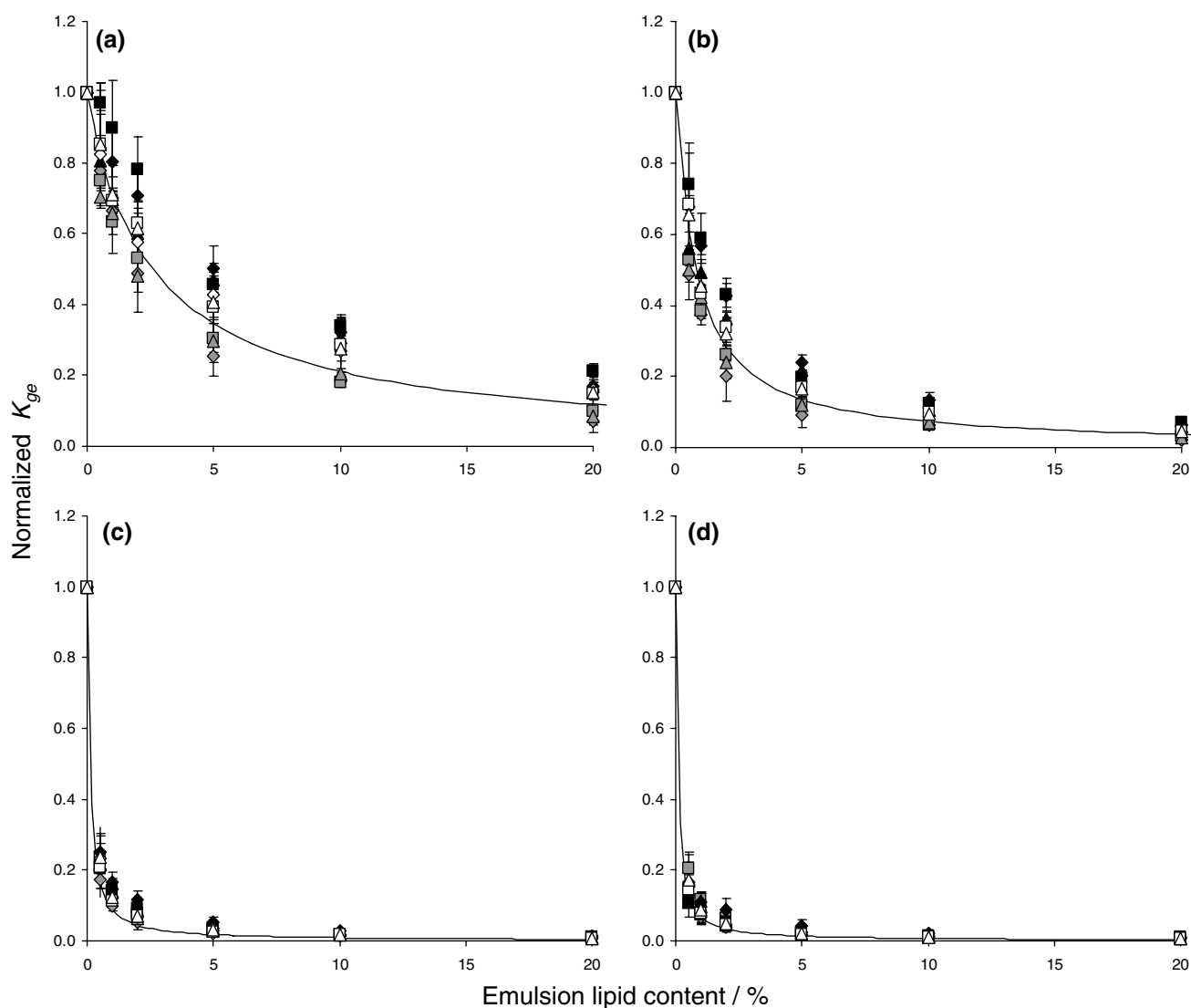


**Fig. 2** Normalized gas–emulsion partition coefficient ( $K_{ge/w}$ ) of aroma compounds as a function of lipid type and lipid content of emulsions with liquid lipid **a** ethyl butanoate, **b** ethyl pentanoate, **c** ethyl heptanoate and **d** ethyl octanoate. Results for emulsions with different particle sizes ( $d_{32}$ ) large (open diamonds), medium (open

squares) and small (open triangles) are shown for *n*-eicosane (open symbols), HPS (closed black symbols) and Salatrim<sup>®</sup> (grey symbols) emulsions. Model prediction using Buttery equation (Buttery et al. [9]) has also been shown by lines

freezing point for several weeks without any measurable crystallization.

#### Equilibrium Aroma Release from Emulsions

The gas–emulsion partition coefficient ( $K_{ge}$ ) was calculated from the HS volatile concentration data for each emulsion assuming that volatiles present in the HS were at equilibrium with the emulsion and that the total amount of aroma compounds added were distributed between the HS and the emulsion. In earlier work, it was shown that the selected volatiles did not measurably interact with sodium caseinate in the emulsion [3].

Because different samples were measured at different temperatures it was necessary to account for the effect of temperature on  $K_{ge}$  before making a comparison between them. This was done by normalizing the measured  $K_{ge}$  to the gas–water partition coefficient at each experimental temperature, i.e.:

$$K_{ge/w} = \frac{K_{ge}}{K_{gw}} \quad (2)$$

Therefore  $K_{ge/w}$  denotes the release of a volatile aroma compound into the HS from an emulsion relative to the release of that compound from water at the same temperature and concentration. By converting  $K_{ge}$  to  $K_{ge/w}$  we

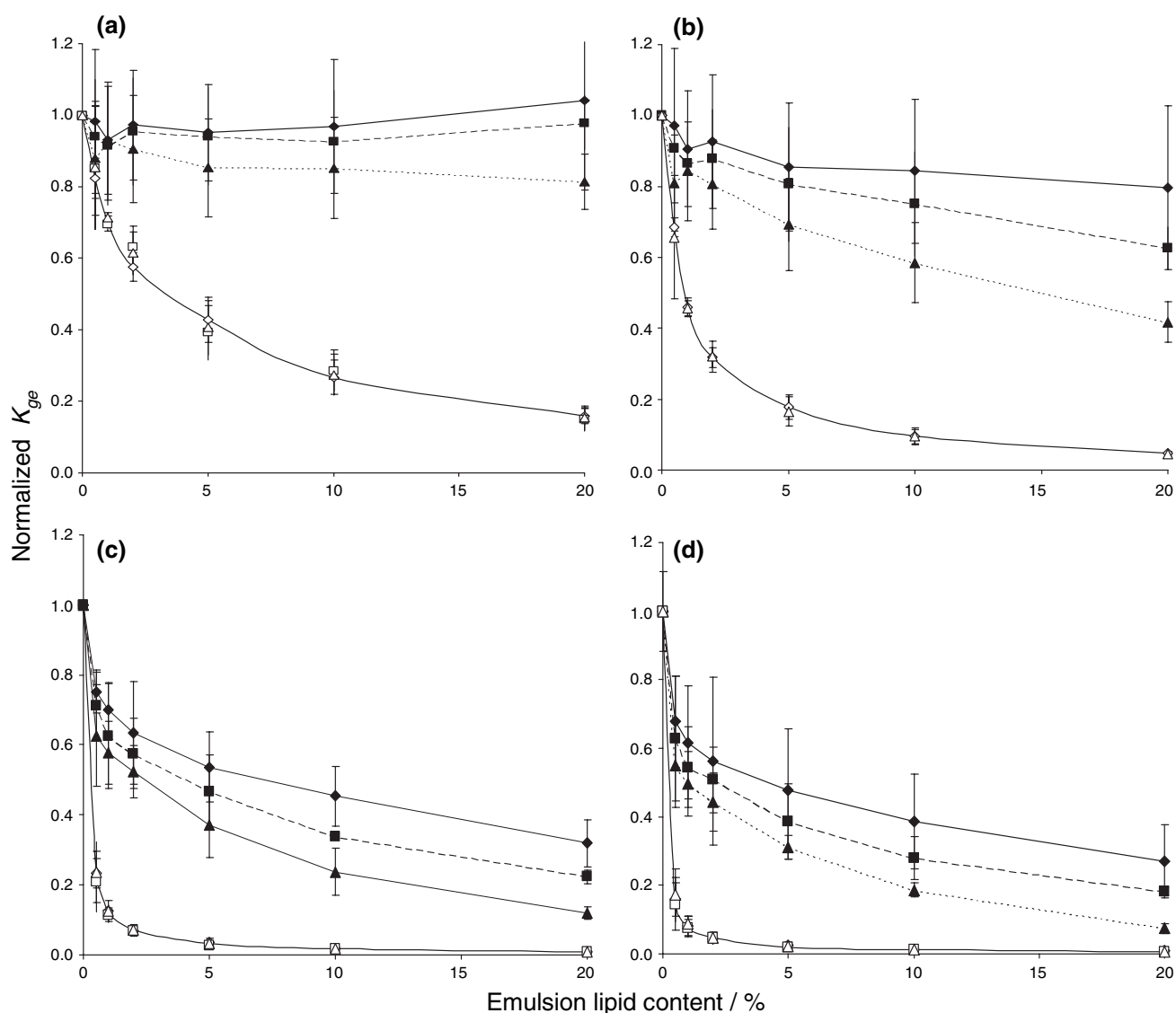


**Fig. 3** Normalized gas–emulsion partition coefficient ( $K_{ge/w}$ ) of aroma compounds as a function of lipid content of emulsions with liquid lipid (open symbols) and solid lipid (closed symbols) droplets **a** ethyl butanoate, **b** ethyl pentanoate, **c** ethyl heptanoate and **d** ethyl octanoate. Results for eicosane emulsions with different particle sizes

( $d_{32}$ ) highest (open diamonds), medium (open squares) and lowest (open triangles) are shown. Solid lipid data points are connected for each particle size while only one line has been used to connect the liquid lipid data points

were able to compare all of the HS GC measurements at different temperatures (according to Table 1) for different lipid emulsions (Figs. 2, 3, 4, 5, 6). This approach has also been used by Roberts et al. [5] to compare relative head-space volatile concentration from emulsions at different temperatures.

#### Aroma Release from Liquid Lipid Emulsions

The calculated values of  $K_{ge/w}$  were plotted as a function of emulsion liquid lipid content and droplet size in Fig. 2.

The partitioning of volatiles into the HS decreased with emulsion lipid content but there were no differences between the types of lipid used (i.e., *n*-eicosane, HPS and Salatrim<sup>®</sup>) or emulsion droplet size. Partitioning in liquid lipid droplets depends on the total volume of the droplets and is therefore a function of the affinity between the lipid and aroma compound and on the amount of lipid but not the droplet size [3]. In this case the amount of aroma partitioning into the emulsion increased with volatile molecular weight but was unaffected by lipid type. This was expected as the gas–oil partition coefficients of alkanes and triglycerides at any particular temperature were very

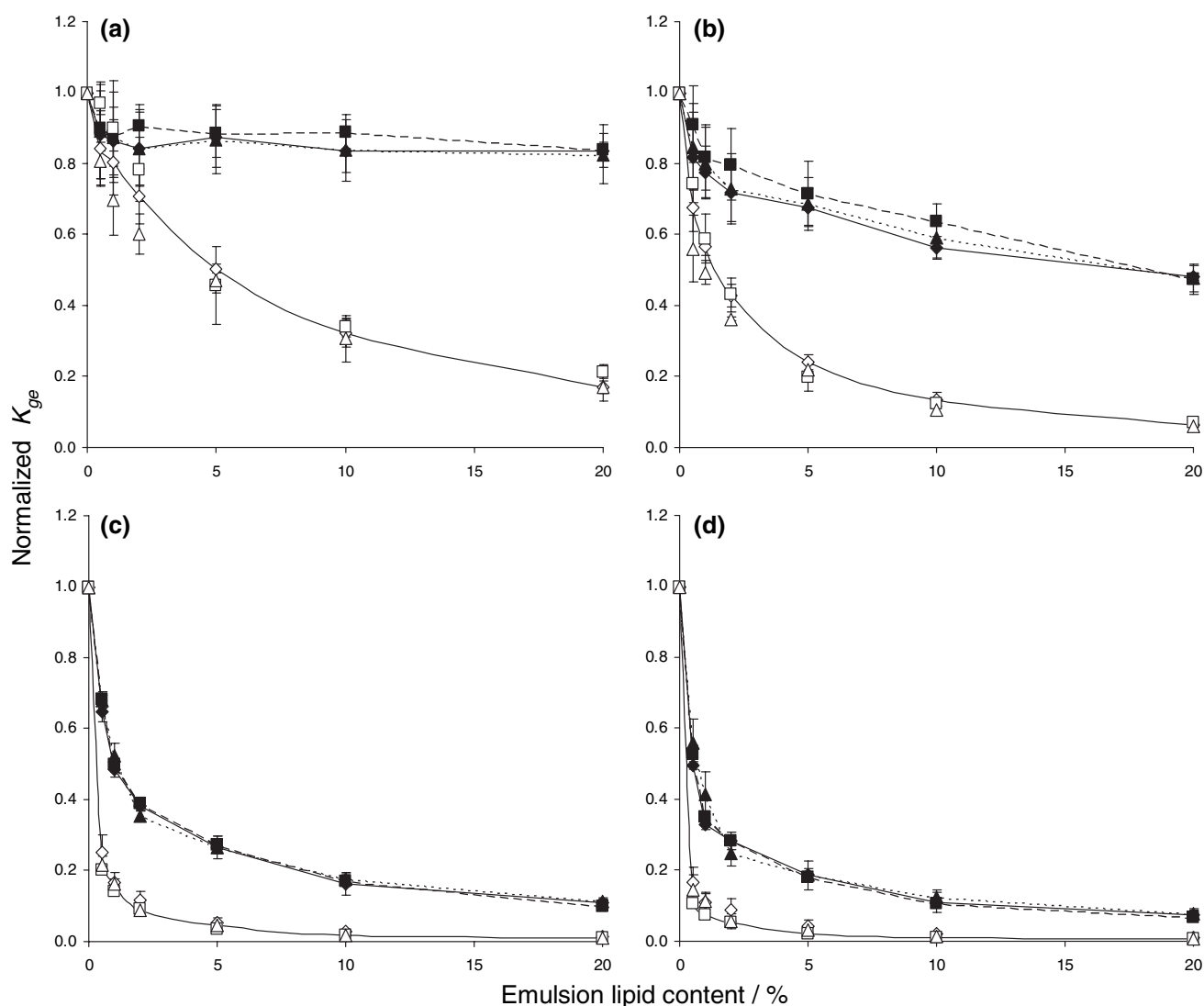


**Fig. 4** Normalized gas–emulsion partition coefficient ( $K_{ge/w}$ ) of aroma compounds as a function of lipid content of emulsions with liquid lipid (open symbol) and solid lipid (closed symbol) droplets **a** ethyl butanoate, **b** ethyl pentanoate, **c** ethyl heptanoate and **d** ethyl octanoate. Results for HPS emulsions with different particle sizes

( $d_{32}$ ) highest (open diamond), medium (open squares) and lowest (open triangles) are shown. Solid lipid data points are connected for each particle size while only one line has been used to connect the liquid lipid data points

similar (Table 2). Indeed all of the liquid droplet data can be well-described by Eq. 1 using these values for the partition coefficients and neglecting any surface binding terms, i.e., the Buttery model [9] (Fig. 2).

#### Aroma Release from Solid Lipid Emulsions

The values of  $K_{ge/w}$  for solid droplet emulsions were higher than those for the corresponding liquid droplet emulsions (Figs. 3, 4, 5) suggesting the interaction between aroma and emulsion is weaker. However, for all lipid types, the  $K_{ge/w}$  values for EP, EH and EO decreased

monotonically with solid lipid concentration, suggesting some sort of association of aroma compounds with the solid lipid (Figs. 3, 4, 5). Regardless of aroma type, the  $K_{ge/w}$  of solid eicosane emulsion was highest followed by solid HPS and solid Salatrim<sup>®</sup> emulsions (Fig. 6). Interestingly, although  $K_{ge/w}$  for EB varied with solid Salatrim<sup>®</sup> droplet concentration in a similar manner to the other aroma compounds, it was not affected by eicosane or HPS solid droplet concentration.

As noted previously [3] the values of  $K_{ge/w}$  for solid droplet eicosane emulsions were lower for small droplets than for large droplets (Fig. 3). It was suggested that as the aroma compounds adsorbed at the solid droplet



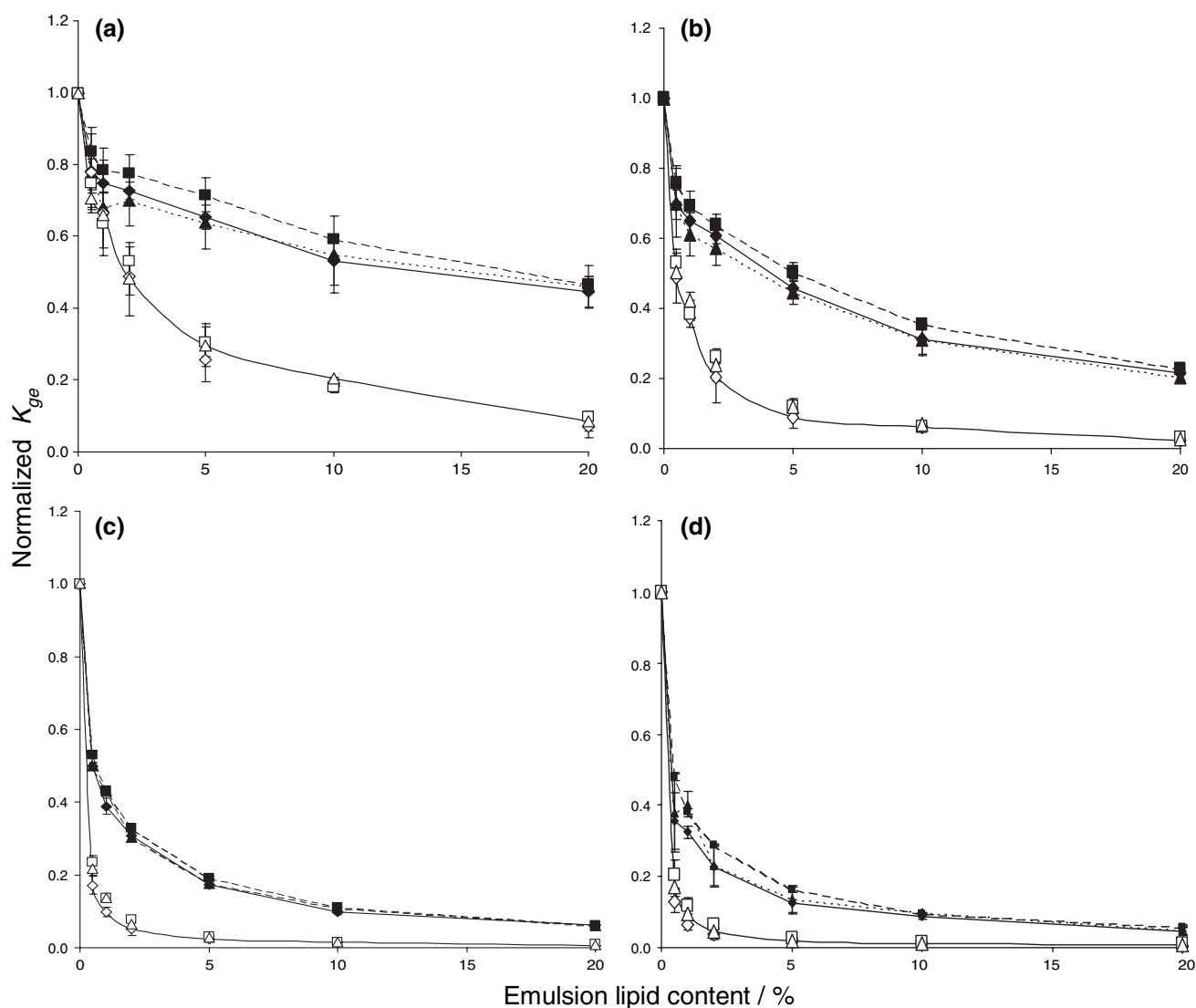


**Fig. 5** Normalized gas–emulsion partition coefficient ( $K_{ge/w}$ ) of aroma compounds as a function of lipid content of emulsions with liquid lipid (open symbols) and solid lipid (closed symbols) droplets **a** ethyl butanoate, **b** ethyl pentanoate, **c** ethyl heptanoate and **d** ethyl octanoate. Results for Salatrim<sup>®</sup> emulsions with different particle

sizes ( $d_{32}$ ) highest (open diamonds), medium (open squares) and lowest (open triangles) are shown. Solid lipid data points are connected for each particle size while only one line has been used to connect the liquid lipid data points

surface, adsorption would be larger for smaller droplets and hence less will be available for partitioning into the HS. Eicosane crystallizes in pure form with tightly arranged aliphatic chains organized in a triclinic crystal structure [10] and presumably with few defects that might accommodate aroma molecules in the crystal lattice. Thus, it is expected that when *n*-eicosane crystallizes, it excludes all aroma compounds from the crystalline matrix. A similar exclusion of foreign materials from crystalline alkane droplets was also postulated by Okuda et al. [11]. They found that the crystallization of *n*-octadecane (which has a similar crystal structure to *n*-eicosane [10]) in mixed octadecane–methyl linolenate oil-in-water

emulsion droplets leads to separation of methyl linolenate from solid octadecane. In the present experiment the extent of surface binding increases with aroma molecular chain length (hydrophobicity). Presumably the lack of a droplet concentration effect of EB (Fig. 3) was because this molecule is relatively hydrophilic and did not tend to associate with the droplet surface.

For the triglyceride emulsions (Figs. 4, 5), the values of  $K_{ge/w}$  decreased with the solid droplet concentration. However, there was no effect of particle size on aroma volatility suggesting that the triglyceride emulsions dependent on phase volume and not on interfacial area. The ineffectiveness of particle size on aroma volatility



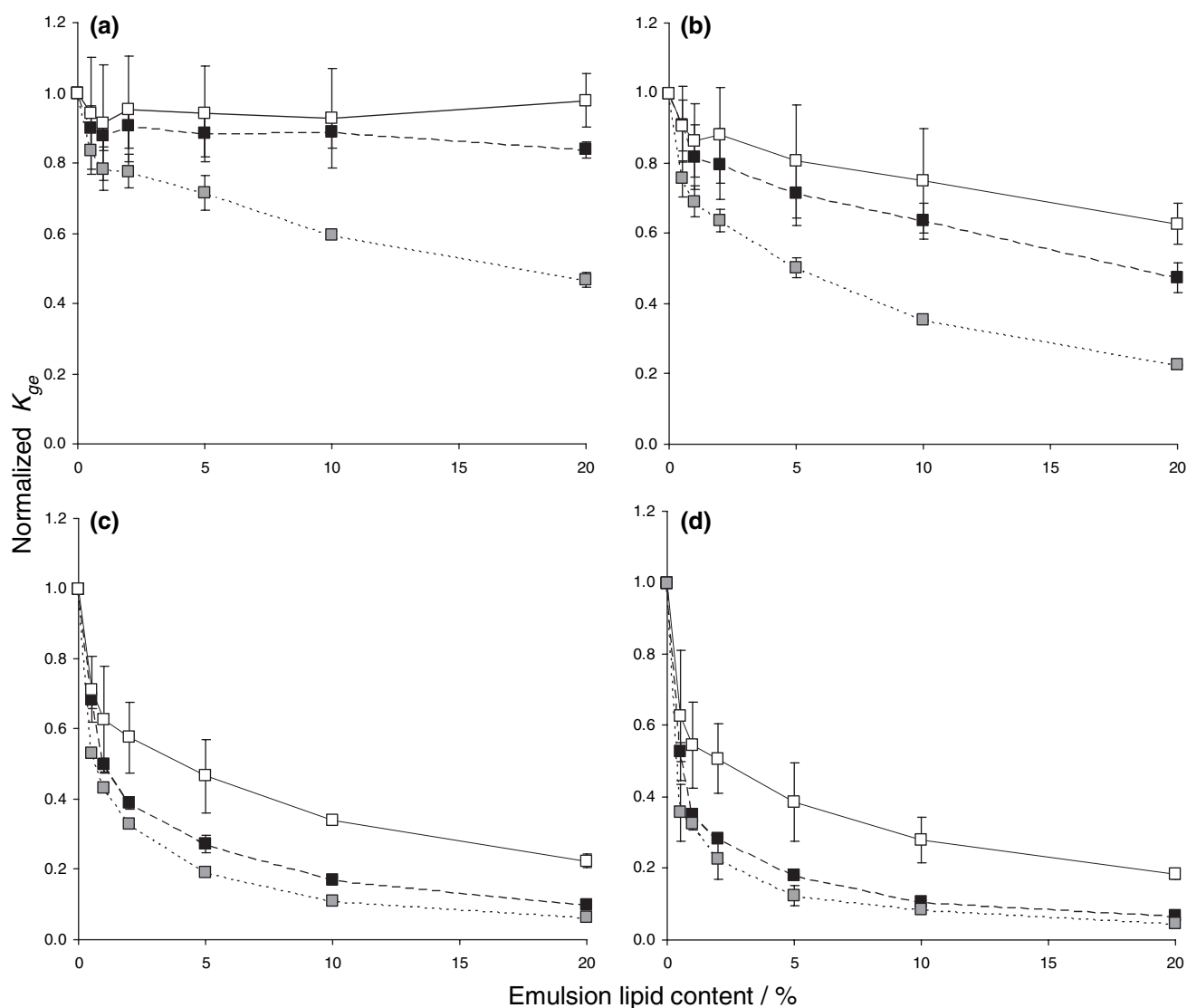


**Fig. 6** Normalized gas–emulsion partition coefficient ( $K_{ge/w}$ ) of aroma compounds as a function of lipid content of emulsions with solid lipid droplets **a** ethyl butanoate, **b** ethyl pentanoate, **c** ethyl

heptanoate and **d** ethyl octanoate. Results for emulsions with different lipid types  $n$ -icosane (open squares), HPF (closed black squares) and Salatrim<sup>®</sup> (grey squares) are shown for  $d_{32} = \sim 0.5 \mu\text{m}$

**Table 2** Gas–oil partition coefficients of aroma compounds at 30 °C

Aroma compounds	Gas–alkane partition coefficient	Gas–triglyceride partition coefficient
Ethyl butanoate	$1.9 \times 10^{-4}$	$1.4 \times 10^{-4}$
Ethyl pentanoate	$6.4 \times 10^{-5}$	$5.6 \times 10^{-5}$
Ethyl heptanoate	$6.5 \times 10^{-6}$	$8.1 \times 10^{-6}$
Ethyl octanoate	$2.2 \times 10^{-6}$	$3.0 \times 10^{-6}$

As bulk eicosane and HPS are solid at the experimental temperatures, hexadecane and corn oil were used as a model alkanes and triglyceride, respectively. The partition coefficients were measured according to the method mentioned by Ghosh et al. [3]

could be either because (1) there is some liquid lipid residual in the “solid” droplet which acts as a reservoir for the aroma, or (2) the aroma compounds co-crystallize with the solid lipid.

#### Residual Liquid Lipid

The first of these proposed mechanisms may be reasonable for the solid Salatrim<sup>®</sup> droplets because, according to the manufacturer, the solid lipid content is only 91% at 10 °C (the measurement temperature). If the residual liquid lipid

is responsible for the interactions of the aroma molecules with the droplets, then the value of  $K_{ge/w}$  for “solid” droplet Salatrim<sup>®</sup> emulsions should be equal to those of a similar liquid droplet emulsion with a lower lipid content. A modified form of the Buttery equation was used to model the data and test this hypothesis [4]:

$$\frac{1}{K_{ge}} = \frac{\phi_o(1 - \phi_{sf})}{K_{go}} + \frac{(1 - \phi_o)}{K_{gw}} \quad (3)$$

where,  $\phi_{sf}$  is solid lipid content of the lipid (taken as 91% for Salatrim<sup>®</sup>). Equation 3 is similar to Eq. 1 with the exception that only the liquid fraction of the lipid was assumed to interact with the emulsion and no surface binding effects were considered. The prediction from the model was shown alongside the data for EH in Fig. 7a ( $r^2 = 0.95$ ). While the trends in the data and the model were similar and the fit is better than the 100% liquid lipid line (also shown) the quantitative fit agreement of theory and experiment was only moderate. The best fit of Eq. 3, shown in Fig. 7a, assumed that the solid lipid content of the solid Salatrim<sup>®</sup> was 95% ( $r^2 = 0.98$ ). The actual value of the solid lipid content of the droplets under the experimental measurement conditions is hard to specify precisely and may differ significantly from the bulk measurements reported by the manufacturer [12]. However, these calculations give an indication that even a small amount of liquid lipid in an apparently solid lipid may be all that is required to bind an appreciable amount of aroma compounds. In the eicosane droplets there was presumably little or no liquid lipid, so the only interactions could be at the surface.

A similar approach was taken for the solid HPS emulsions and the best fit between theory and experiment was obtained for a solid lipid content of 97% (Fig. 7b). The theoretical line fitted the experimental data well ( $r^2 = 0.98$ ), but how reasonable was the assumption that there was 3% liquid lipid in these samples? HPS has a capillary melting point of 60 °C (from the supplier specifications) and we do not expect any liquid to be present in the pure lipid at 10 °C but perhaps the presence the aroma compounds formed a liquid aroma-lipid solution phase at the lipid crystal grain boundaries. The presence of liquid lipid at the grain boundaries was shown in the images included in Marangoni's recent book [13]. In this case, the partitioning of the aroma into the solid lipid droplets depended on the phase behavior of the aroma-lipid system and the volumes of the phases and not on the droplet size.

#### Co-crystallization

An alternative mechanism for the interaction between solid lipid and aroma compounds is the co-crystallization of two

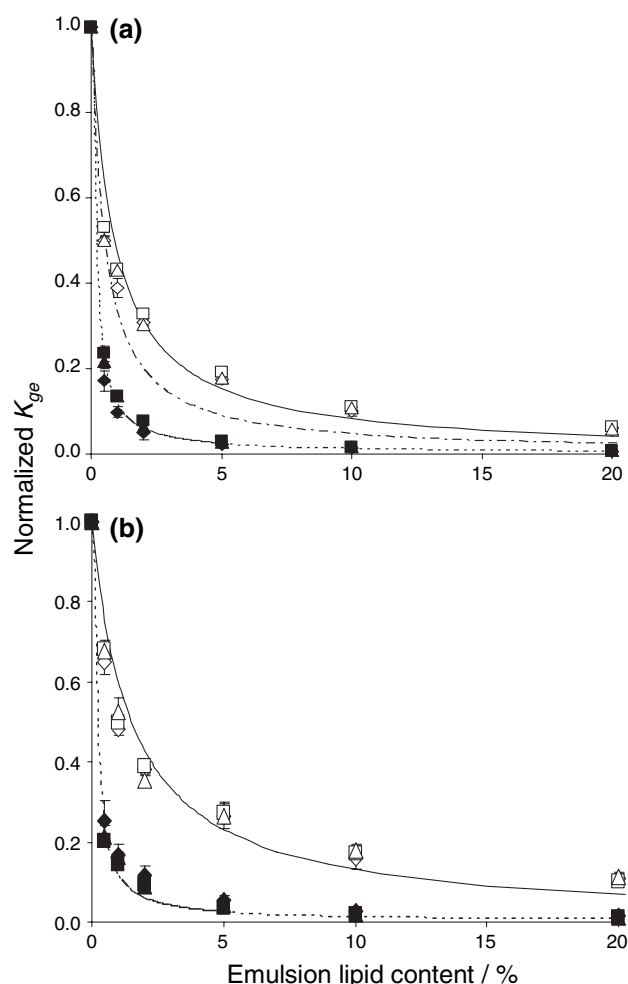


**Fig. 7** Normalized gas–emulsion partition coefficient ( $K_{ge/w}$ ) of ethyl heptanoate (EH) as a function of lipid content of emulsions with solid lipid droplets. Data for **a** Salatrim<sup>®</sup> and **b** HPS emulsions with different particle sizes ( $d_{32}$ ) highest (open diamonds), medium (open squares) and lowest (open triangles) are shown along with the model (Eq. 3) predicted line for **a** 9% (dashed dotted line), 5% (dashed line) and **b** 3% (dashed line) liquid lipid content. The gas–oil and gas–water partition coefficients values of EH were taken as  $8.1 \times 10^{-6}$  and  $1.82 \times 10^{-2}$ , respectively. Also shown pure liquid lipid emulsion data (closed black symbols) and theoretical prediction (dotted line) from Buttery model (Buttery et al. [9])

chemicals. Although, aroma partitioning from emulsified triglycerides can be explained from their liquid lipid content, there are structural differences that might also explain aroma partitioning. Emulsified HPS crystallized into a mixture of unstable  $\alpha$  and more stable  $\beta/\beta'$  polymorphs (Fig. 1b). The aliphatic chains of crystalline triglycerides are disordered in the  $\alpha$  form, packed with an intermediate density in the  $\beta'$  form and most densely packed in the  $\beta$  form [14]. It has been proposed that because of lower packing density,  $\alpha$  crystals would be able to support a greater load of co-crystallized solute [15, 16]. Therefore, it is expected that solid HPS droplets would be able to

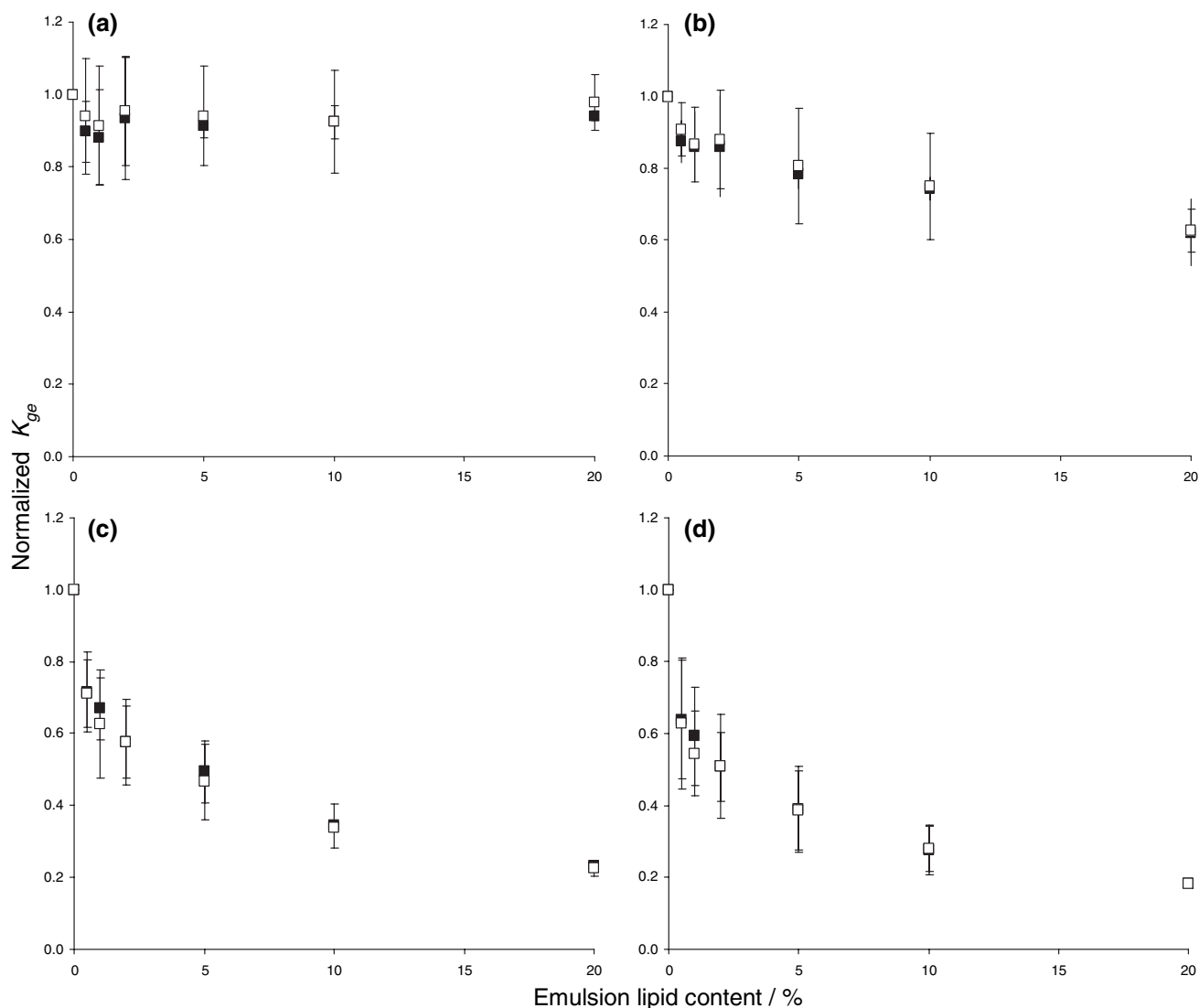


**Fig. 8** Normalized gas–emulsion partition coefficient ( $K_{ge/w}$ ) of aroma compounds as a function of lipid content of eicosane emulsions ( $d_{32} \sim 0.5 \mu\text{m}$ ) with solid lipid droplets comparing Solid I (open

symbols) and recrystallized Solid II (closed symbols) samples **a** ethyl butanoate, **b** ethyl pentanoate, **c** ethyl heptanoate and **d** ethyl octanoate

accommodate some aroma compounds into their crystalline matrices and on their surfaces by adsorption. Thus the HS aroma concentration would be lower than that of the *n*-eicosane emulsion. A similar argument was used in reference to the incorporation of a drug into solid lipid nanoparticles [16]. Drug molecules would be excluded from the lipids forming crystals with perfect lattices (e.g., monoacid triglycerides) [17] whereas the molecules would be incorporated into less perfect crystal structures of complex triglycerides [16].

Salatrim<sup>®</sup> has a highly asymmetrical molecular structure and hence packing into a definite crystalline polymorph is difficult [18, 19]. Narine et al. [18] proposed that the solid phase of Salatrim<sup>®</sup> is characterized by random arrangement

of platelet-like growth. This type of growth would lead to more surface area in solid Salatrim<sup>®</sup> droplets compared to HPS droplets and hence space for more aroma adsorption. The situation is somewhat similar to the physical structure of co-crystallized flavor and sugar agglomerates where flavor molecules are included between numerous micro-sized irregular sugar crystals [20, 21].

#### Reversibility of Aroma–Solid Lipid Interaction

Solid I samples were prepared by adding a stock aroma solution to solid droplet emulsions. However, if the aroma molecules were present in liquid lipid droplets

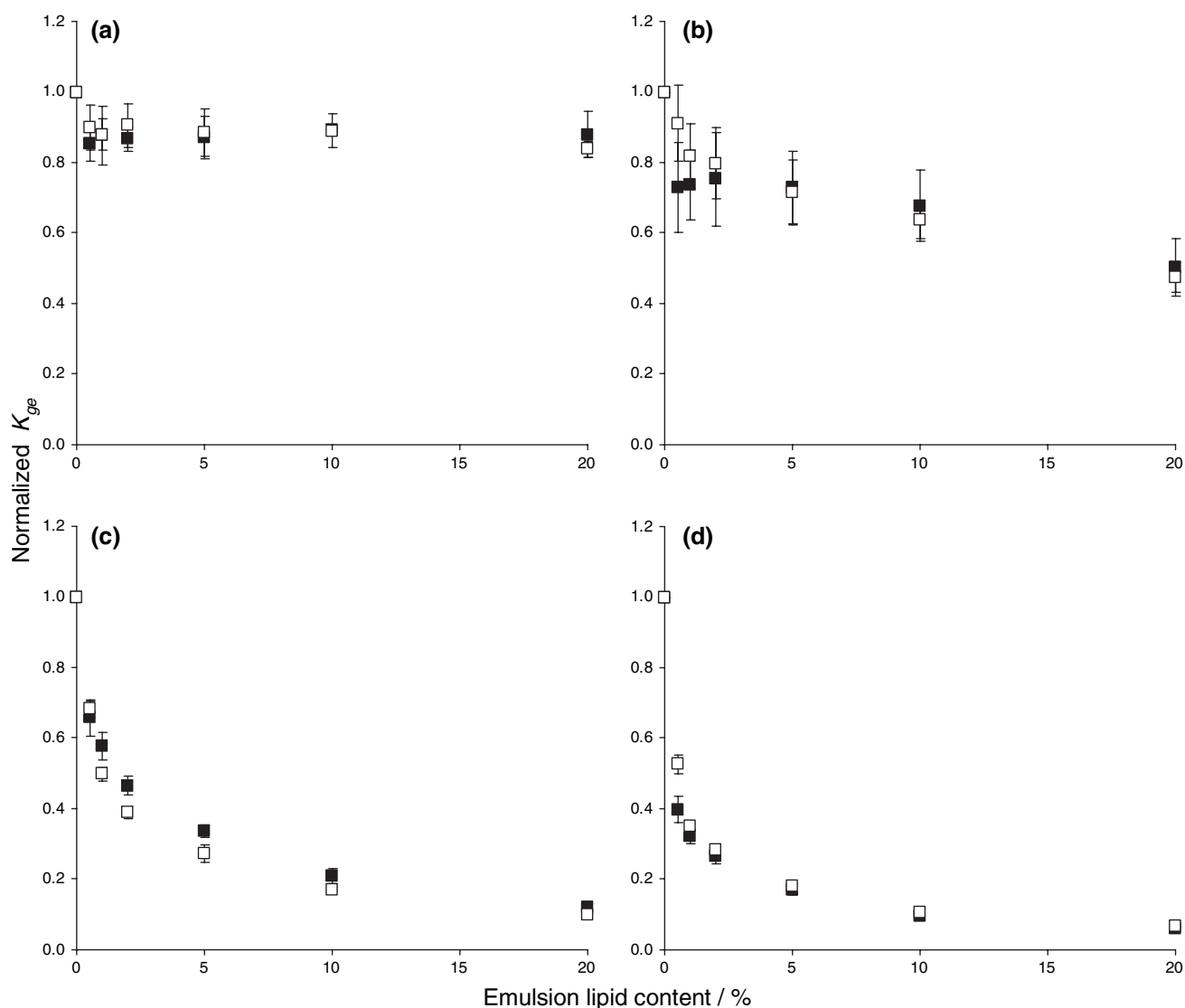


**Fig. 9** Normalized gas–emulsion partition coefficient ( $K_{ge/w}$ ) of aroma compounds as a function of lipid content of HPS emulsions ( $d_{32} \sim 0.5 \mu\text{m}$ ) with solid lipid droplets comparing Solid I (open

symbols) and recrystallized Solid II (closed symbols) samples **a** ethyl butanoate, **b** ethyl pentanoate, **c** ethyl heptanoate and **d** ethyl octanoate

before fat crystallization, will they be entrapped inside the crystalline solid lipids? To test this hypothesis, Solid II samples were prepared by melting the aroma added solid droplet emulsions followed by re-crystallization of liquid droplet emulsions and  $K_{ge/w}$  were measured. The partitioning behavior of Solid I and Solid II samples were similar irrespective of lipid type (Figs. 8, 9, 10). This indicated that at equilibrium the amount of aroma incorporated into the solid phase or adsorbed on the solid lipid surface was constant and defined by the thermodynamic properties of the phases. There was no evidence of any “entrapment” of volatiles within the crystal droplet.

## Conclusion

The partitioning of volatile aroma compounds was dependent on the composition of the system (oil concentration, aroma type) but not on the type of liquid lipid used in the emulsions. Interactions between solid lipid droplets and hydrophobic aroma compounds were much weaker than those with liquid lipid droplets but were significantly influenced by the nature of the solid lipid. *n*-Alkanes, crystallized in pure form and excluded all aroma compounds from the solid droplets (although some can adsorb to the droplet surfaces). Aroma compounds also interacted with complex triglyceride mixtures in food lipids but the

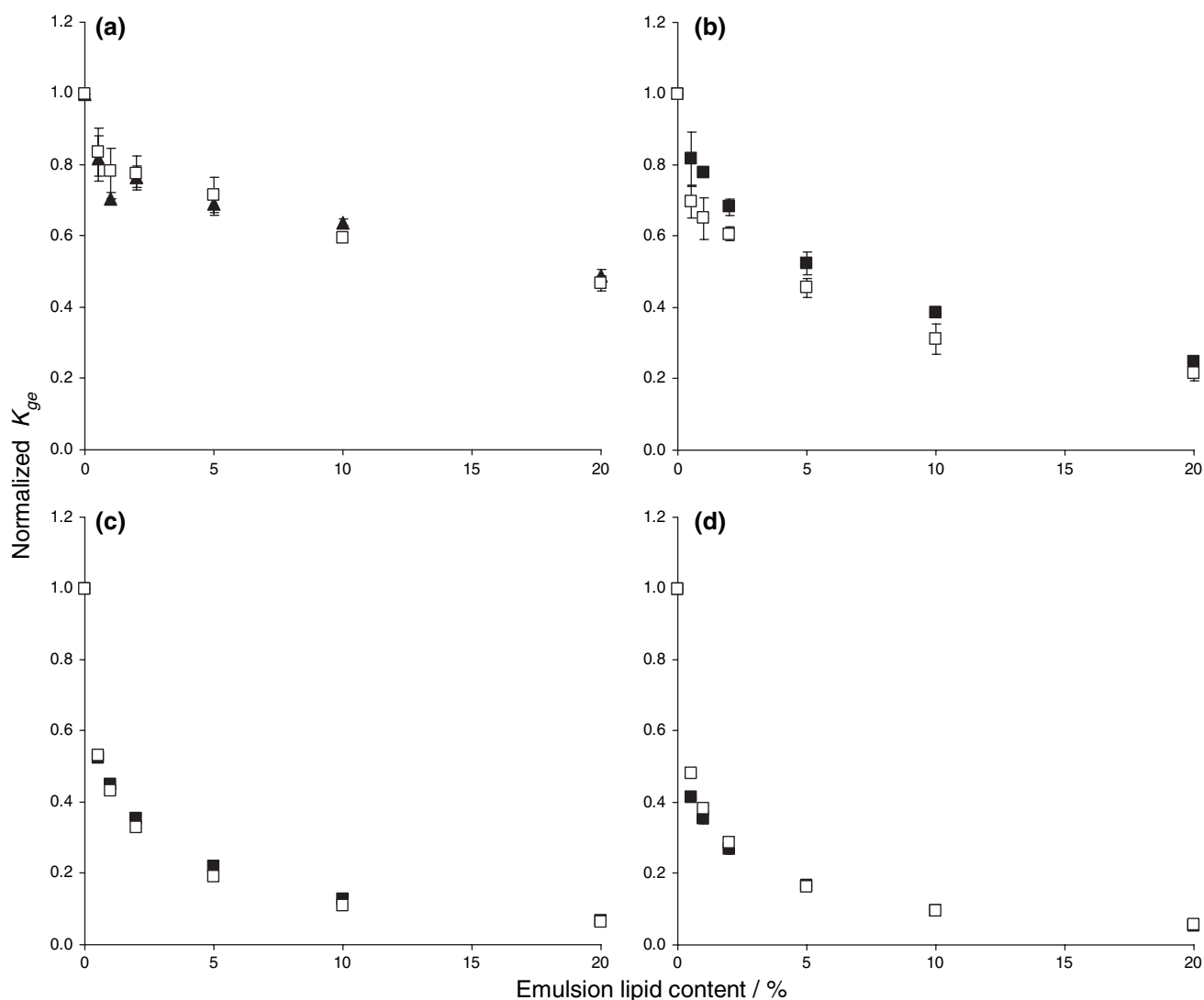


**Fig. 10** Normalized gas–emulsion partition coefficient ( $K_{ge/w}$ ) of aroma compounds as a function of lipid content of Salatrim<sup>®</sup> emulsions ( $d_{32} \sim 0.5 \mu\text{m}$ ) with solid lipid droplets comparing Solid I

(open symbols) and recrystallized Solid II (closed symbols) samples **a** ethyl butanoate, **b** ethyl pentanoate, **c** ethyl heptanoate and **d** ethyl octanoate

mechanism of interaction was different and dependent on the volume not the surface area of the droplets. This could be explained by the presence of residual liquid lipid at the crystal grain boundaries in the “solid” droplet which acted as a reservoir for the aroma. Alternatively, as triglycerides crystallized in a mixture of different polymorphs, their less perfect crystal structure might allow the co-crystallization of aroma compounds.

## References

1. Keast RSJ, Dalton PH, Breslin PAS (2004) Flavor interaction at the sensory level. In: Taylor AJ, Roberts DD (eds) Flavor perception. Blackwell, Oxford, pp 228–249
2. Taylor AJ (1996) Volatile flavor release from foods during eating. *Crit Rev Food Sci Technol* 36:765–784
3. Ghosh S, Peterson DG, Coupland JN (2006) Effects of droplet crystallization and melting on the aroma release properties of a model oil-in-water emulsion. *J Agric Food Chem* 54:1829–1837
4. Ghosh S, Peterson DG, Coupland JN (2007) Flavor binding by solid and liquid emulsion droplets. In: Dickinson E, Leser M (eds) Food colloids: self assembly and material science. Royal Society of Chemistry, Cambridge
5. Roberts DD, Pollien P, Watzke B (2003) Experimental and modelling studies showing the effect of lipid type and level on flavor release from milk-based liquid emulsions. *J Agric Food Chem* 51:189–195
6. McNulty PB, Karel M (1973) Factors affecting flavor release and uptake in O/W emulsions. 2. Stirred cell studies. *J Food Technol* 8:319–331
7. Kloek W, Walstra P, van Vliet T (2000) Nucleation kinetics of emulsified triglyceride mixtures. *J Am Oil Chem Soc* 77:643–652

8. Coupland JN (2002) Crystallization in emulsions. *Curr Opin Colloid Interface Sci* 7:445–450
9. Buttery RG, Guadagni DG, Ling LC (1973) Flavor compounds: volatilities in vegetable oil and oil–water mixtures. Estimation of odor thresholds. *J Agric Food Chem* 21:198–201
10. Ueno S, Hamada Y, Sato K (2003) Controlling polymorphic crystallization of n-alkane crystals in emulsion droplets through interfacial heterogeneous nucleation. *Cryst Growth Des* 3:935–939
11. Okuda S, McClements DJ, Decker EA (2005) Impact of lipid physical state on the oxidation of methyl linolenate in oil-in-water emulsions. *J Agric Food Chem* 53:9624–9628
12. Dickinson E, McClements DJ (1995) *Advances in food colloids*. Chapman & Hall, New York
13. Litwinenko JW (2005) Fat crystal network: microstructure DVD image archive. In: Marangoni AG (ed) *Fat crystal networks*. Marcel Dekker, New York
14. Sato K (2001) Crystallization behavior of fats and lipids—a review. *Chem Eng Sci* 56:2255–2265
15. Bunjes H, Koch MHJ (2005) Saturated phospholipids promote crystallization but slow down polymorphic transitions in triglyceride nanoparticles. *J Control Release* 107:229–243
16. Muller RH, Mader K, Gohla S (2000) Solid lipid nanoparticles (SLN) for controlled drug delivery—a review of the state of the art. *Eur J Pharm Biopharm* 50:161–177
17. Westesen K, Bunjes H, Koch MHJ (1997) Physicochemical characterization of lipid nanoparticles and evaluation of their drug loading capacity and sustained release potential. *J Control Release* 48:223–236
18. Narine SS, Marangoni AG (1999a) The difference between cocoa butter and Salatrim lies in the microstructure of fat crystal network. *J Am Oil Chem Soc* 76:7–13
19. Narine SS, Marangoni AG (1999b) Microstructure and rheological studies of fat crystal network. *J Cryst Growth* 198/199:1315–1319
20. Chen AC, Veiga MF, Rizzuto AB (1988) Co-crystallization—an encapsulation process. *Food Technol* 42:87–90
21. Zeller BL, Saleeb FZ (1996) Production of microporous sugars for adsorption of volatile flavors. *J Food Sci* 61:749